

# The Impact of Temperature & Pressure on Borehole Fluids Density



Jianglin Zhu<sup>1</sup>, Zhaoyong Wang<sup>2\*</sup>, Gang Liu<sup>2</sup>, Jianxiong Wei<sup>3</sup> and Jiangjian Song<sup>4\*</sup>

<sup>1</sup>Southern Marine Science and Engineering Guangdong Laboratory (Zhanjiang), China

<sup>2</sup>China Oilfield Services Ltd. Blue Ocean BD Hi-Tech Co. Ltd, China

<sup>3</sup>School of Materials Science and Engineering, South China University of Technology, China

<sup>4</sup>Key Laboratory of Drilling and Production Engineering for Oil and Gas, China

Submitted: December 12, 2022; Published: June 12, 2026

\*Corresponding author: Zhaoyong Wang, China Oilfield Services Ltd. Blue Ocean BD Hi-Tech Co. Ltd, Quanzhou 362800, PR, China

Jiangjian Song, Key Laboratory of Drilling and Production Engineering for Oil and Gas, Hubei Province, Wuhan 430100, PR, China

## Abstract

The balanced cementing is one of the most important measures to ensure the well cementing quality. Borehole fluids expand with the formation heating and compress with the fluid column pressure, which causes variations of the borehole fluids density. Inadequate choose of injected fluids density can easily cause the pressure unstable because of the narrow safety pressure window, big temperature difference & pressure difference of deep wells and high temperature & high-pressure wells. By the self-developed HTHP fluids density variation gauge, the author has measured the density variation curves of water, spacer fluids, cement slurry and mineral oil affected by temperature and pressure, and selected the suitable density model for the temperature & pressure variation of cement slurry. This paper mainly introduces the operating mechanism and experimental phenomena of the self-developed gauge, and then calculates the static equivalent density curves of water-base and oil-base mud with different injecting density under the condition of different down-hole geothermal gradients, providing references for the density design of drilling and cementing fluids of deep wells and high temperature & high-pressure wells.

**Keywords:** Temperature; Pressure; Borehole fluids; Density variation; Cementing design; Drillbench software

**Abbreviations:** RBF: Radial Basis Function; MLP: Multilayer Perceptron; LSSVM: Least Square Support Vector Machine; GA: Genetic Algorithm; ICA: Competitive Algorithm; PSO: Particle Swarm Optimization; PVT: Pressure-Volume-Temperature; ESD: Equivalent Static Density; HTHP: High-Temperature and High-Pressure

## Introduction

Many difficulties are encountered during drilling and well completion in high-temperature and high-pressure (HTHP) environments. One such challenge is that the density of the drilling fluid and cement slurry is not constant but changes with temperature and pressure [1]. Predicting the true density of a downhole working fluid has become a key issue in the design and construction of drilling and cementing to prevent blowout and leakage in HTHP wells within a narrow pressure window [2].

Due to technical difficulties and high economic and time costs in measuring the actual densities of drilling and completion fluids under high temperatures and high pressures, integrated algorithms and models for drilling fluid prediction have been proposed, including linear empirical analytical, correlation and

intelligent approaches. In particular, Adamson et al. reported the effect of high temperature and high pressure on the drilling fluid density as the source of the wellbore instability in HTHP wells [3]. Kutasov proposed a model with empirically regression coefficients for determining the density of downhole drilling fluids [4] at the University of Texas calculated the effect of the drilling fluid density on the downhole pressure based on a component model for the drilling fluid density [5] proposed a density model for pure and mixed-salt brines [6] studied the effects of temperature and pressure on the density of water- and diesel-based drilling fluids [7]. used a materials balance approach to develop a composition prediction model for the density of water- and diesel-based drilling fluids, i.e., a so-called "composite model" [8]. However, different components of the drilling fluid (water, oil and the solid

phase) must be separately tested to determine the respective rules before the model can be applied. Application of this model is thereby restricted. Babu at the Indian Oil Corporation, Limited used an empirical model for the drilling fluid density to determine the effect of changes in the drilling fluid density on the static pressure but produced an evidently problematic formula [9]. Wang at the SINOPEC Petroleum Exploration and Production Research Institute developed an empirical model for the drilling fluid density [10]. This model does not distinguish between the effects of oil and water on the density and was not validated by experimental data. Intelligent models have been proposed in recent years, such as the radial basis function (RBF) [11-13], multilayer perceptron (MLP) [14,15] and least square support vector machine (LSSVM) based on the original model of Suykens [16,17], genetic algorithm (GA) [18], imperialist competitive algorithm (ICA) [19], particle swarm optimization (PSO) [20] and

composite models thereof. A variety of density models have been used for oil- and water-based drilling fluid systems worldwide, but a cement slurry model has not been developed. Therefore, the objective of this study was to design an instrument for measuring the drilling fluid density in a well at a specific temperature and pressure and to use the obtained data to develop an appropriate density model for a drilling fluid and cement slurry.

### Experimental Instruments, Principles and Methods

#### Experimental instruments

Figure 1 shows the instrument designed to measure changes in the density of a bottomhole fluid in HTHP environments. The three main components of the instrument are a tank, a temperature control system and a pressure-volume-temperature (PVT) pressure control system.

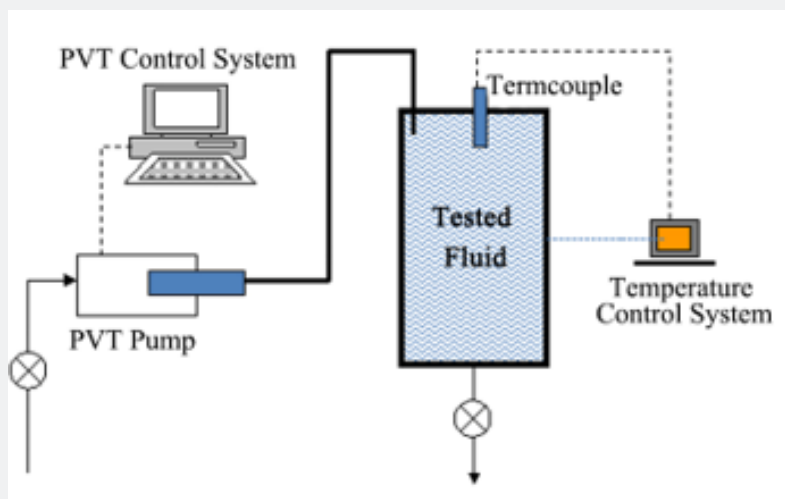


Figure 1: Schematic of the instrument designed for measuring changes in the fluid density in an HTHP environment.

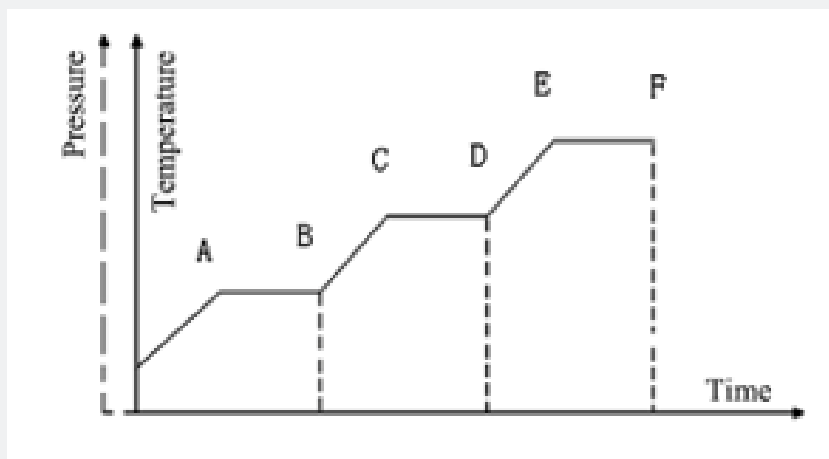


Figure 2: Schematic of the experimental method.

The tank is used to hold the fluid sample to be tested and provide a closed HTHP-resistant environment.

The main components of the temperature control system are a 7040 thermostat and a temperature sensor. The experimental scheme consists of using different heating durations and target temperatures to simulate the downhole environmental temperature.

The main components of the PVT pressure control system are a PVT pump and a PVT data acquisition system. The PVT pump accurately controls the tank pressure through the displacement of a piston, and the PVT data acquisition system accurately measures the volume change of the fluid that drives the piston under a given pressure.

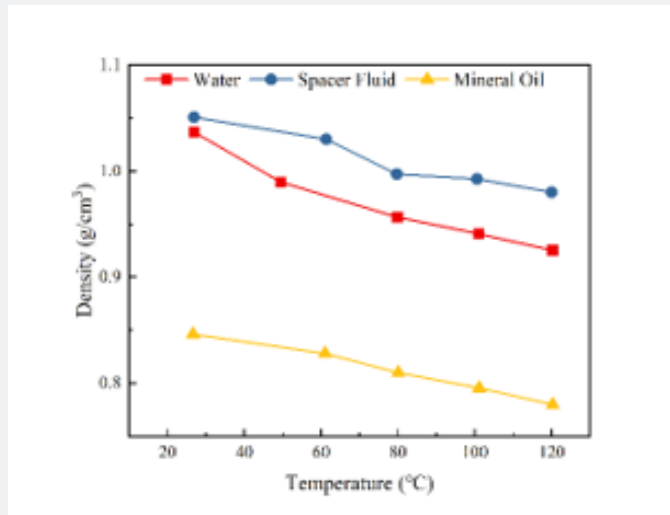


Figure 3: Effect of temperature on the fluid density.

**Experimental principle**

Changes in the volume of the test fluid in the tank with the temperature and pressure cause the PVT piston to move. The computer control system calculates the volume of the outflow/inflow of the tank through a displacement sensor. The corresponding change in the weight of the fluid for a fixed tank volume (250ml) was used to calculate the density of the fluid at this temperature and pressure as given below.

That is,

$$\rho_1 = \frac{\rho_0 v_0 - \rho_1 \Delta v}{v_0} \quad (1)$$

$$\rho_1 = \frac{\rho_0 v_0}{v_0 + \Delta v} \quad (2)$$

where

$\rho_0$  — Initial density of the fluid at the ground surface

$V_0$  — Tank volume

$\rho_1$  — Downhole fluid density

$\Delta V$  — Density of the fluid in the inflow/outflow of the tank

**Experimental method**

- i. The test fluid is fed into the tank. If the test fluid is a cement slurry or weighted mud, a small quantity of water should be added to the top of the tank.
- ii. The temperature control system is used to set the temperature at different test points following the same procedure used to test the compressive strength of a cement slurry, as shown in Figure 2. The temperature at each test point should be maintained for more than 30 minutes (e.g., the length of time between A and B should be greater than 30 minutes) to ensure that all the fluid in the tank is heated to the same temperature. Tests are performed by increasing the fluid temperature from low to high. Figure 2 Schematic of the experimental method
- iii. The test pressures at different test temperature points are set by the pressure control system.
- iv. At the end point of each constant-temperature test segment (B, D and F in Figure 2), the inflow and outflow volumes of the tank are recorded.
- v. The density at each end point is calculated according to Equation (2).

**Analysis of the Effects of Temperature and Pressure on the Fluid Density**

**Effect of temperature on the fluid density**

Changes in the densities of the spacer fluid, fresh water and mineral oil were determined at different temperatures and a fixed pressure of 6.89MPa. The test results presented in Figure 3 show that temperature affected the densities of the three fluids to different extents. Increasing the temperature from 20°C to 120°C resulted in a decrease in the densities of the spacer fluid, fresh water and mineral oil of 5.58%, 7.3% and 7.76%, respectively.

**Effect of pressure on the fluid density**

Changes in the densities of the spacer fluid, fresh water and mineral oil were determined at different pressures and a fixed temperature of 30°C. The initial densities of the spacer fluid and the mineral oil were 1.04 g/cm<sup>3</sup> and 0.85 g/cm<sup>3</sup>, respectively. The test results presented in Figure 4 indicate that the pressure affected the density of the three fluids to different extents. Increasing the pressure from atmospheric to 63MPa resulted in a decrease in the densities of spacer fluid, fresh water and mineral oil of 13%, 17.6% and 7.7%, respectively.

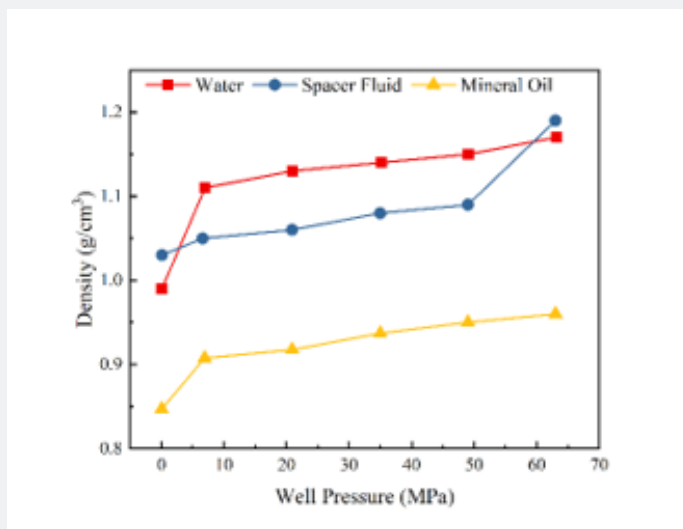


Figure 4: Effect of pressure on the fluid density.

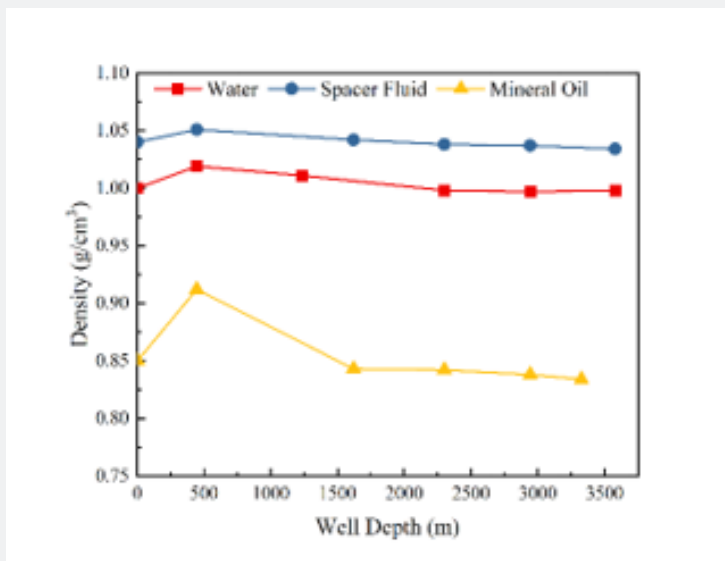
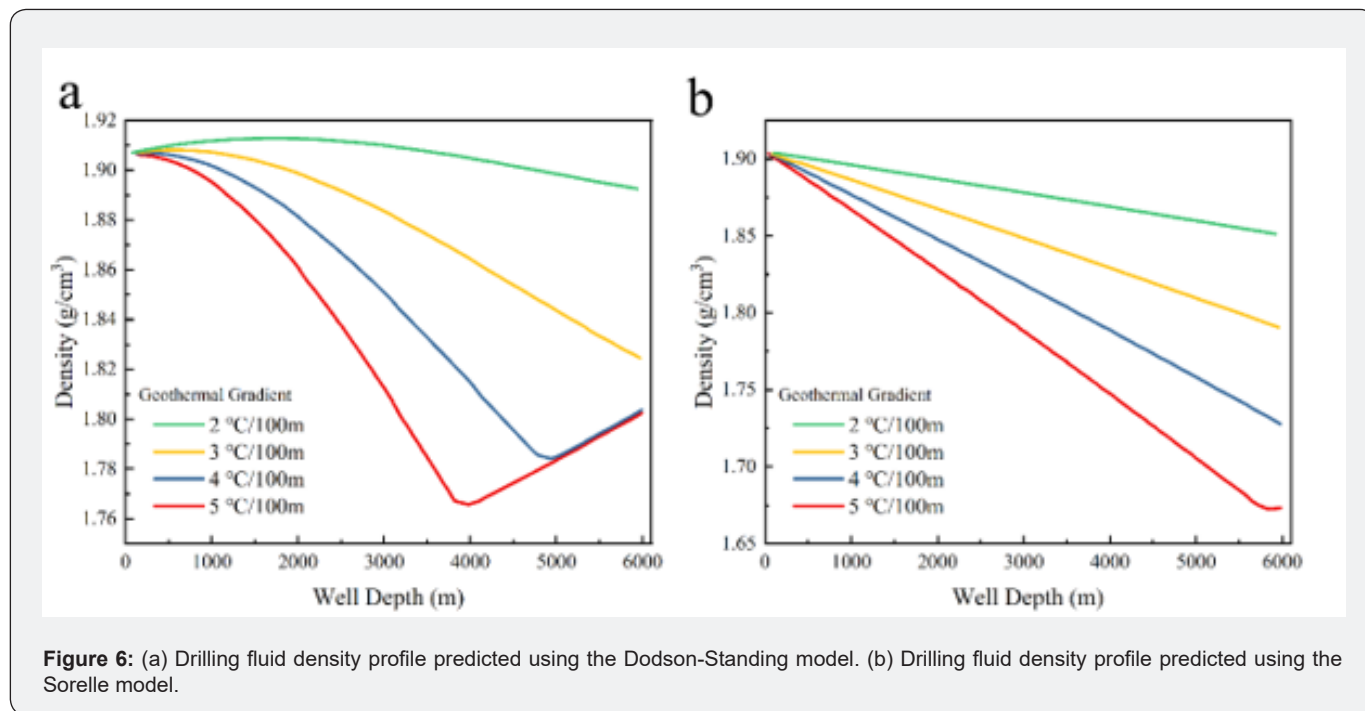


Figure 5: Relationship between the densities of downhole fluids and the well depth.

**Effect of temperature and pressure on the fluid density**

Tests were performed on the spacer fluid, fresh water and mineral oil using the procedure described in Table 9.12 of the

Procedure for Testing Well Cements (GB/T 19139-2003) with a geothermal gradient of 3.5°C/100 m [21] and the test conditions shown in Table 1. The test results are shown in Table 1 and Figure 5.



**Figure 6:** (a) Drilling fluid density profile predicted using the Dodson-Standing model. (b) Drilling fluid density profile predicted using the Sorelle model.

**Table 1:** Effects of the temperature and pressure on the densities of downhole fluids.

| Well Depth (M) | Temperature (°C) | Pressure (MPa) | Fresh Water (g/cm <sup>3</sup> ) | Spacer Fluid (g/cm <sup>3</sup> ) | Mineral Oil (G/cm <sup>3</sup> ) |
|----------------|------------------|----------------|----------------------------------|-----------------------------------|----------------------------------|
| 0              | 20               | 0.1            | 1                                | 1.04                              | 0.85                             |
| 445            | 27               | 7.2            | 1.019                            | 1.051                             | 0.912                            |
| 1237           | 50               | 20             | 1.011                            |                                   |                                  |
| 1620           | 62               | 26.2           |                                  | 1.042                             | 0.843                            |
| 2300           | 81               | 37.2           | 0.998                            | 1.038                             | 0.842                            |
| 2944           | 101              | 47.6           | 0.997                            | 1.037                             | 0.838                            |
| 3327           | 112              | 53.8           |                                  |                                   | 0.834                            |
| 3580           | 120              | 57.9           | 0.998                            | 1.034                             |                                  |

The test results showed that as the well depth increased from 0 m to 2,944m, the densities of the spacer fluid, fresh water and mineral oil decreased by 0.288%, 0.30% and 1.4%, respectively, under the combined effect of temperature and pressure.

**Selection of a cement grout density model**

Drillbench software has been used to establish a PVT model, a heat-transfer model and a flow model to describe the variation in the drilling fluid density with the temperature and pressure. Three density models have been established for water-based fluids: the Dodson-Standing, Kemp-Thomas and Sorelle models. These models produce quite different predictions. Figure 6 show

the density of a water-based drilling fluid (with a density of 1.9 g/cm<sup>3</sup> at the surface temperature of 20°C) calculated using the Dodson-Standing and Sorelle models, respectively.

Table 2 is a comparison of the experimental results and the model predictions, showing that the Dodson-Standing model is more suitable than the Sorelle model for describing a cement slurry under downhole conditions.

**Effect of the geothermal gradient and initial inflow fluid density on the equivalent static density (ESD)**

Drillbench software has been used to establish four density models for oil-based fluids: the Standing, Glass, Sorelle and Table

models. The Sorelle (oil) model is recommended among these models.

Figure 7 & 8 show the results of using the Sorelle (oil) and Dodson-Standing models to calculate the ESD of fluids with different initial inflow fluid densities. Figure 7 & 8 show that at

the lower the drilling fluid density and the higher the geothermal gradient are, the larger the impact of the temperature and pressure on the density is. Table 3 shows that changes in temperature and pressure produce larger density changes in oil-based drilling fluids than in water-based drilling fluids.

**Table 2:** Comparison of cement slurry densities obtained by experimental measurements and different models.

| Well Depth (m) | Bottomhole Temperature (°C) | Bottomhole Pressure (MPa) | Outflow Volume (ml) | Measurement                  |                              | Dodson-Standing Model                   |                              | Sorelle Model                           |                              |
|----------------|-----------------------------|---------------------------|---------------------|------------------------------|------------------------------|---|------------------------------|---|------------------------------|
|                |                             |                           |                     | Density (g/cm <sup>3</sup> ) | Density Ratio $\gamma$ : (%) | Calculated Density (g/cm <sup>3</sup> ) | Density Ratio $\gamma_2$ (%) | Calculated Density (g/cm <sup>3</sup> ) | Density Ratio $\gamma_3$ (%) |
| 0              | 20                          | 0.1                       | 0                   | 1.895                        | 0                            | 1.9                                     | 0                            | 1.9                                     | 0                            |
| 1000           | 50                          | 18.6                      | -3.03               | 1.914                        | 101                          | 1.902                                   | 101                          | 1.887                                   | 99.3                         |
| 2000           | 80                          | 37.3                      | 0.65                | 1.889                        | 99.7                         | 1.894                                   | 99.7                         | 1.868                                   | 98.3                         |
| 3000           | 110                         | 55.8                      | 2.71                | 1.87                         | 98.7                         | 1.878                                   | 98.8                         | 1.85                                    | 97.4                         |

**Table 3:** Comparison of the effect of the density and geothermal gradient on the reduction in the fluid ESD.

| Well Depth (M) | BHST (°C) | Density Changes at 1.2 g/cm <sup>3</sup> (%) |           | Density Changes at 1.8 g/cm <sup>3</sup> (%) |           | Density Changes at 2.0 g/cm <sup>3</sup> (%) |           |
|----------------|-----------|--|-----------|--|-----------|--|-----------|
|                |           | Water-Based                                  | Oil-Based | Water-Based                                  | Oil-Based | Water-Based                                  | Oil-Based |
| 0              | 20        | 0  | 0         | 0  | 0         | 0  | 0         |
| 3000           | 170       | 2.66   | 3.66      | 1.83   | 2.6       | 1.55   | 2.39      |
| 4000           | 220       | 4.25   | 5.08      | 3  | 3.61      | 2.55   | 3.3       |
| 5000           | 270       | 5.58   | 6.41      | 3.8  | 4.6       | 3.3  | 4.14      |
| 6000           | 320       | 6.16   | 8.4       | 4.2  | 5.6       | 3.55   | 4.94      |

**Note:** The geothermal gradient is 5°C/100m.

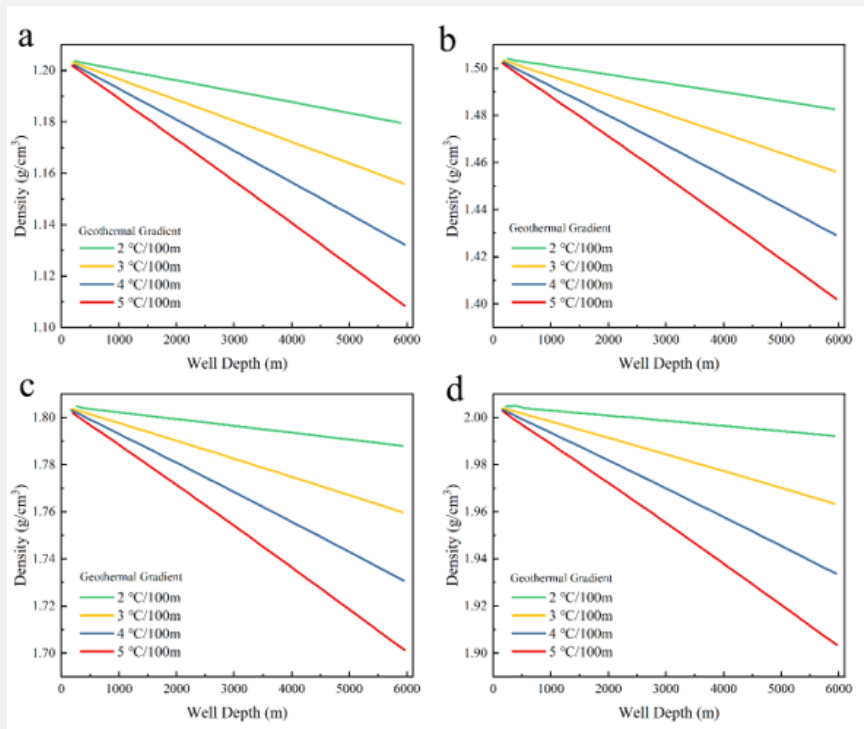


**Figure 7:** (a) ESD of oil-based mud at 1.2sg. (b) ESD of oil-based mud at 1.5sg. (c) ESD of oil-based mud at 1.8sg. (d) ESD of oil-based mud at 2.0sg.

## Test results and discussion

i. The initial inflow fluid density can be selected from Figures 8 to 15 based on the formation equivalent density and the types of drilling and completion fluids.

ii. To calculate the stable pressure for HTHP cementing, the effective residual pressure should be calculated using the actual density in the well considering temperature and pressure effects.

## Conclusion

i. A set of methods for evaluating changes in the fluid density in HTHP environments has been established, and a test instrument with high operability has been designed.

ii. Temperature and pressure have quite different effects on water-based fluids than oil-based fluids. For both water- and oil-based drilling fluids, the actual fluid density in deep wells decreases with increasing well depth, and the fluid density in the upper well segment is slightly higher at low geothermal gradients than at high geothermal gradients.

iii. The lower the drilling fluid density and the higher the geothermal gradient are, the larger the impact of the temperature and pressure on the density is. Changes in the temperature and pressure produce larger density changes in oil-based drilling fluids than in water-based drilling fluids.

iv. As the well depth increases from 0 m to 5,000 m at 250 °C, the densities of water- and oil-based muds decrease by 5.58% and 6.4%, respectively.

v. The Dodson-Standing model is suitable for evaluating the effect of temperature and pressure on the density of a cement slurry.

vi. The downhole ESD map calculated by Drillbench software can be used to select the initial inflow fluid density that stabilizes the formation pressure.

## References

1. Alizadeh SM, Alrueyemi I, Daneshfar R, Khanaposhtani MM, Naseri M (2021) An insight into the estimation of drilling fluid density at HPHT condition using PSO-, ICA-, and GA-LSSVM strategies. *Sci Rep* 11(1): 7033.
2. Syah R, Ahmadian N, Elveny M (2021) Implementation of artificial intelligence and support vector machine learning to estimate the drilling fluid density in high-pressure high-temperature wells. *Energy Reports* 7: 4106-4113.
3. Kutasov IM (1988) Empirical correlation determines downhole mud density. *Oil & Gas Journal* 86(50): 61-63.
4. Peter EJ (1991) Oilmud: A Microcomputer program for predicting oil-based mud densities and static pressure. *SPE Drilling Engineering* 6(1): 57-59.
5. Kemp NP (1987) Density Modeling for Pure and Mixed-Salt Brines as a Function of Composition Temperature and Pressure. *SPE/IADC Drilling Conference*.
6. McMordie WC, Bland RG, Hauser JM (1982) Effect of Temperature and Pressure on the Density of Drilling Fluids *SPE* 11114.
7. Hoberock LL, et al. (1982) Bottom Hole Mud Pressure Variations Due to Compressibility and Thermal Effects: *IADC Drilling Technology Conference, Houston, USA*.
8. Babu DR (1996) Effect of Mud Behavior on Static Pressure During Deep Well Drilling. *SPE Drilling & Completion* 11(2): 91-97.
9. Haige W, Minghui H, Liping Y (2000) The P-p-T (pressure-density-temperature) behavior of HPHT drilling fluid and its effect on wellbore pressure calculation. *Oil Drilling & Production Technology* 22(1):17-21.
10. Kardani MN (2019) Phase behavior modeling of asphaltene precipitation utilizing RBF-ANN approach. *Pet Sci Technol* 37(16): 1861-1867.
11. Rahmati AS, Tatar A (2019) Application of Radial Basis Function (RBF) neural networks to estimate oil field drilling fluid density at elevated pressures and temperatures. *Oil Gas Sci Technol Revue d'IFP Energies Nouvelles* 74: 50.
12. Kardani N, Zhou A, Nazem M, Lin X (2021) Modelling of municipal solid waste gasification using an optimized ensemble soft computing model. *Fuel* 289:119903.
13. Daneshfar R, Farhad K, Khanaposhtani M, Mohammad, Alireza B (2020) A neural computing strategy to estimate dew-point pressure of gas condensate reservoirs. *Pet Sci Technol* 38(10): 706-712.
14. Daneshfar R, Bemani A, Hadipoor M, Sharifpur M, Ali HM, et al. (2021) Estimating the heat capacity of non-Newtonian ionanofluid systems using ANN, ANFIS, and SGB tree algorithms. *Appl Sci* 10(18): 6432.
15. Ahmadi MA (2016) Toward reliable model for prediction drilling fluid density at wellbore conditions: A LSSVM model. *Neurocomputing* 211: 143-149.
16. Rostami S, Rashid F, Safari H (2019) Prediction of oil-water relative permeability in sandstone and carbonate reservoir rocks using the CSA-LSSVM algorithm. *Petrol Sci Eng* 173: 170-186.
17. Mohammadi M, Khorrami MM, Vatani L, Ghasemzadeh H, Vatanparast H, et al. (2020) Genetic algorithm-based support vector machine regression for prediction of SARA analysis in crude oil samples using ATR-FTIR spectroscopy. *Spectrochim Acta Part A Mol Biomol Spectrosc* 245: 118945.
18. Ahmadi MA, Ebadi M, Shokrollahi A, Majidi SMJ (2013) Evolving artificial neural network and imperialist competitive algorithm for prediction oil flow rate of the reservoir. *Appl Soft Comput* 13(2): 1085-1098.
19. Ahmadi MA, Soleimani R, Lee M, Kashiwao T, Bahadori A (2015) Determination of oil well production performance using artificial neural network (ANN) linked to the particle swarm optimization (PSO) tool. *Petroleum* 1(2): 118-132.
20. Ashrafi SB, Anemangely M, Sabah M, Ameri MJ (2019) Application of hybrid artificial neural networks for predicting rate of penetration (ROP): A case study from Marun oil field. *Petrol Sci Eng* 175: 604-623.
21. GB/T 19139-2003 Procedure for testing well cements.



This work is licensed under Creative Commons Attribution 4.0 License  
DOI: [10.19080/JOJMS.2026.10.555797](https://doi.org/10.19080/JOJMS.2026.10.555797)

**Your next submission with JuniperPublishers  
will reach you the below assets**

- Quality Editorial service
- Swift Peer Review
- Reprints availability
- E-prints Service
- Manuscript Podcast for convenient understanding
- Global attainment for your research
- Manuscript accessibility in different formats  
**( Pdf, E-pub, Full Text, Audio )**
- Unceasing customer service

**Track the below URL for one-step submission**  
<https://juniperpublishers.com/submit-manuscript.php>